Importance of the Adaptor (Membrane Fusion) Protein Hairpin Domain for the Functionality of Multidrug Efflux Pumps†

Johannes F. Stegmeier, Georg Polleichtner, Nicolas Brandes, Christian Hotz, and Christian Andersen*

Universität Würzburg, Lehrstuhl für Biotechnologie, Biozentrum der Universität Würzburg, Am Hubland, D-97074 Würzburg, Germany

Received February 15, 2006; Revised Manuscript Received July 3, 2006

ABSTRACT: Drug efflux pumps of Gram-negative bacteria are tripartite export machineries located in the bacterial envelopes contributing to multidrug resistance. Protein structures of all three components have been determined, but the exact interaction sites are still unknown. We could confirm that the hybrid system composed of *Pseudomonas aeruginosa* channel tunnel OprM and the *Escherichia coli* inner membrane complex, formed by adaptor protein (membrane fusion protein) AcrA and transporter AcrB of the resistance nodulation cell division (RND) family, is not functional. However, cross-linking experiments show that the hybrid exporter assembles. Exchange of the hairpin domain of AcrA with the corresponding hairpin from adaptor protein MexA of *P. aeruginosa* restored the functionality. This shows the importance of the MexA hairpin domain for the functional interaction with the OprM channel tunnel. On the basis of these results, we have modeled the interaction of the hairpin domain and the channel tunnel on a molecular level for AcrA and TolC as well as MexA and OprM, respectively. The model of two hairpin docking sites per TolC protomer corresponding with hexameric adaptor proteins was confirmed by disulfide cross-linking experiments. The role of this interaction for functional efflux pumps is discussed.

Multidrug resistance (MDR)[1] has become a growing problem in the medical treatment of pathogenic bacteria (*1*). In Gram-negative bacteria, multidrug efflux pumps play an important role in resistance by expelling antimicrobial agents and thus reducing their concentration in the cells (*2*). Hence, they may increase antibiotic resistance by several orders of magnitude, rendering antibiotics clinically useless (*3*). An important group of multidrug efflux pumps is based on a tripartite assembly, which is composed of an outer membrane exit duct of the TolC family, an energized inner membrane transporter, and a periplasmic adaptor protein, also known as a membrane fusion protein (*4*, *5*). These subunits, each members of an extensive protein family, are thought to assemble into a transporter unit during export of the substrates to span both the inner and outer membrane and create a bridge across the periplasm. Crystal structures of proteins belonging to any of the involved families are known. Trimeric outer membrane proteins TolC of *Escherichia coli* and OprM of *Pseudomonas aeruginosa* are representatives of channel tunnels, forming a canon-shaped hollow conduit, which is anchored in the outer membrane by a β-barrel, the channel domain, and protrude into the periplasm with a 100 Å long α-barrel, the tunnel domain (*6*, *7*). AcrB of *E. coli* is the first crystallized member of the RND (resistance nodulation cell division) transporter family (*8*). It also forms trimers, which look like jellyfish. The 50 Å thick membrane-embedded part has a diameter of 80 Å. Periplasmic loops form the headpiece protruding 70 Å into the periplasm. The headpiece is divided into two stacked parts. The bottom part is called the pore domain. In its center is a cavity, which is connected laterally with the periplasm by three openings, which might serve as conduits for substrate entry. The upper part of the cavity is linked by a central pore with a funnel-like structure characterizing the top part of the headpiece. Recently, a direct interaction between the rim of the funnel and the periplasmic end of the channel tunnel could be detected by site-directed disulfide cross-linking (*9*). The third component, the adaptor proteins, is also essential for a functional efflux pump. Whereas the inner and outer membrane proteins could be crystallized in their native oligomerization state, members of the adaptor protein family, MexA of *P. aeruginosa* and AcrA of *E. coli*, crystallized as a tridecamer and a dimer of dimers, respectively, which represents most likely not the native form of the proteins (*10*−*12*). However, in parts the structure of the monomers verified the former structural model of adaptor proteins (*13*) showing a 47 Å long α-helical hairpin domain connected to a flattened β-sandwich domain folded like the already known lipoyl domain from biotinyl/lipoyl carrier proteins. Besides these already predicted domains, a third domain, the α/β-domain, could be determined, showing a six-stranded β-barrel with a short α-helix. It is expected that at least a fourth

† This work was supported by the Deutsche Forschungsgemeinschaft (Emmy Noether fellowship, Grant AN373/1-3).

* To whom correspondence should be addressed. Phone: +49-931-888-4510. Fax: +49-931-888-4509. E-mail: andersen@biozentrum.uni-wuerzburg.de.

[1] Abbreviations: RND, resistance nodulation cell division; MDR, multidrug resistance; MCS, multicloning site; GST, gluthathione *S*-transferase; IPTG, isopropyl β-D-thiogalactopyranoside; SDS, sodium dodecyl sulfate; LB, Luria-Bertani; DSP, dithiobissuccinimidyl propionate; PMSF, phenylmethanesulfonyl fluoride; NTA, nitrilotriacetic acid; DDT, dithiothreitol; AHT, anhydrotetracycline; EDTA, ethylenediaminetetraacetic acid; MIC, minimal inhibitory concentration.

10.1021/bi060320g CCC: $33.50 © 2006 American Chemical Society
Published on Web 08/03/2006

domain comprising the N- and C-terminus of the protein exists because the structure of the 28 N-terminal and 101 C-terminal residues could not be determined (*11*).

All models of multidrug efflux pumps propose that adaptor proteins mediate contact of the RND transporter with the outer membrane channel tunnel (*10*, *11*, *14*). Biochemical experiments have supported this hypothesis showing that AcrA and TolC can be cross-linked, independent of the presence of any externally added substrate (*15*). For the AcrAB−TolC and MexAB−OprM efflux pumps, pull-down assays showed that all three proteins form a tight association (*16*, *17*). With regard to the assembly of drug efflux pumps, the question of which domains of the adaptor protein are necessary for functional interaction with the channel tunnel is open. Gerken and Misra have shown that point mutations in the α/β-domain of AcrA could reverse the hypersusceptible phenotype of a TolC mutant, which suggests that this region might have direct contact with the channel tunnel (*18*).

In this study, we have investigated the impact of the hairpin domain for the interaction of the periplasmic adaptor protein and the outer membrane channel tunnel. We have established a genetic background uncoupling the expression of multidrug efflux compounds from cellular regulation. Via chemical cross-linking, we could show that a hybrid efflux pump assembles even when it is not functional. Functionality could be restored by the exchange of the hairpin domain of the adaptor protein. A model for the interaction of adaptor proteins with channel tunnels is presented.

MATERIALS AND METHODS

Bacterial Strains, Plasmids, and Culture Conditions. All bacterial strains were grown at 37 °C in LB medium or on LB agar plates with appropriate antibiotics (Sigma). Ampicillin (100 μg/mL), kanamycin (50 μg/mL), and chloramphenicol (40 μg/mL) were used for selection of plasmids in *E. coli* strains Top10F′ (Invitrogen), AG100, and DC14 (*19*). *E. coli tolC* knockout strains AG100TC and DC14TC (this work) were grown with reduced antibiotic concentrations (50 μg/mL ampicillin, 25 μg/mL kanamycin, and 10 μg/mL chloramphenicol).

The *tolC* knockout in AG100 and DC14 was performed following the method of Datsenko and Wanner (*20*) using a knockout fragment produced by PCR with the primer pair TolC-KO_up and TolC-KO_down and pKD3 as a template (for all primers, see the Supporting Information). The loss of *tolC* was verified by PCR. The resulting strains were denoted AG100TC and DC14TC, respectively.

Plasmids were constructed using standard recombinant DNA techniques (*21*). PCRs were performed using Pfu Turbo DNA polymerase according to the manufacturer's manual, and DNA was purified using the Nucleospin Extract Kit (Macherey & Nagel). Plasmids were isolated using the Nucleospin Plasmid Kit (Macherey & Nagel). All DNA-modifying enzymes were supplied by MBI Fermentas or New England Biolabs. All constructed plasmids were verified by DNA sequencing (SEQLAB).

Initially, an NdeI cutting site was introduced into pGEX-3X (Amershan Biosciences) in front of the GST gene by QuikChange PCR using the primer pair pGEX_Nde_QC_up and -down. The pNB-pre vector is the product of the ligation of the SalI- and PagI-digested PCR product using the primer pair NB_ACYC_up and NB_ACYC_down and pACYC184 as a template and the NcoI- and XhoI-digested PCR product using the primer pair NB_Gex_up and NB_Gex_down and pGEX-3XNdeI as a template. A multi-cloning site (MCS) cassette with a 5′ CCGG overhang formed by MCS_NB_up and MCS_NB_down was inserted into the XmaI/CIAP (calf intestine alkaline phosphatase)-digested pNB-pre vector. The orientation of the MCS cassette was verified by DNA sequencing, and the resulting plasmids were denoted pNB1 and pNB2, respectively. These expression vectors comprise the origin of replication (p15rep) and the Cm resistance gene (*cat*) of pACYC184 (*22*), the *lacI*^{q} gene, the tac promoter, and the glutathione *S*-transferase (GST) gene of pGEX-3X (Amersham Biosciences) as well as a MCS following the GST gene with cutting sites for SalI, PstI, SacI, XhoI, BglII, AflII, HindIII, and XmaI (order corresponds to the orientation in pNB1).

The pNB vectors are used to express the channel tunnels. The *tolC* gene was first amplified using the primers TolC_up and TolC_down and cloned into pBADMyc/His$_C$ using NcoI/EcoRI. The resulting pBADtolC vector was used as a template for amplifying *tolC* linked to the Myc/His sequence using the primers TolC_NB_up and TolC_NB_down. *tolC*-(Myc/His) was cloned into pNB1 and pNB2 using restriction endonucleases NdeI and XhoI. pNB2oprM was constructed after amplification of *oprM* with primers OprM_up and OprM_down and ligated into a NdeI/HindIII-digested pNB2tolC vector leading to *oprM* connected to the Myc/His sequence.

For disulfide cross-linking experiments, *tolC* was amplified using pBADtolC as a template with the primer pair pASKTolCup and pASKTolCdown and cloned into the pASK-IBA12 vector using BsaI. The resulting pASK-TolC vector carrying the wild-type *tolC* gene with an N-terminal OmpA leader sequence and Strep-tag II was used as a template for cysteine mutations introduced by QuikChange PCR with the primer pairs TolC_S124C_QCup and -down and TolC_S339C_QCup and -down.

The primers AcrAB_up and -down were used to amplify *acrAB*, and the PagI/XhoI-digested PCR product was inserted into the NcoI/XhoI-digested pBADHis$_C$ vector, resulting in pBADacrAB. For disulfide cross-linking experiments, the *bla* resistance gene of pBADacrAB was replaced with the *cat* gene of pACYC184. Therefore, the *cat* gene was amplified from pACYC184 with the primers Cat_BspHI_up and Cat_BspHI_down. The PCR product and the pBADacrAB vector were digested with PagI and ligated, resulting in pBADacrAB-cat.

For the construction of AcrA mutants, *acrA* was cloned into an AflIII/HindIII-digested pUC18 vector using the primers AcrAB_up and AcrA_down for NcoI/HindIII restriction sites. pUC18acrA serves as a template for the introduction of the cysteine mutation by QuikChange PCR using the primer pair AcrA_A93C_QCup and -down and for the one-step hairpin sequence deletion of *acrA* via QuikChange PCR using the primers dHP_up and dHP_down (*23*). For exchange of the AcrA hairpin against the MexA hairpin, the hairpin sequence of *mexA* was amplified using AcrAMexAHP_up and AcrAMexAHP_down as primers. The PCR product itself was used as a primer pair for a QuikChange PCR of pUC18acrA. *acrA*Δ*HP*, *acrAMex*-

AHP, and the AcrA cysteine mutant were excised by Bpu1102I digestion and inserted into the Bpu1102I-digested pBADacrAB vector, resulting in pBADacrABΔHP, pBADacrABMexAHP, and pBADacrA$_{A93C}$B-cat, respectively.

Determination of the Minimal Inhibitory Concentration. The bacterial strains were grown overnight in LB medium supplemented with 50 μg/mL ampicillin and 10 μg/mL chloramphenicol. Afterward, the cultures were diluted into 5 mL of fresh LB medium supplemented with 50 μg/mL ampicillin, 10 μg/mL chloramphenicol, 0.1 μM IPTG, and 0.01% arabinose and grown for 3 h at 37 °C. The cultures were diluted and added to a 96-well-plate (Cellstar) using an initial concentration of 100 cells/well. In every well, 25 μg/mL ampicillin, 5 μg/mL chloramphenicol, 0.1 μM IPTG, 0.01% arabinose, and antimicrobial agents at the following concentrations were given: 0, 2.5, 5.0, 7.5, 10, 15, 20, 40, 60, 80, 100, 120, 150, 180, 210, 240, and 270 μg/mL novobiocin, 0, 4.7, 9.4, 18.8, 25, 37.5, 50, 75, 100, 150, 200, and 300 μg/mL erythromycin, 0, 7.8, 15.6, 31.3, 62.5, 93.8, 125, 187.5, 250, 375, 500, and 750 μg/mL rhodamine 6G, 0, 0.6, 1.3, 2.5, 4.1, 5, 8.1, 10, 16.3, 20, 32.5, and 40 μg/mL benzalkonium chloride, and 0, 1.25, 2.5, 5, 10, 12.5, 20, 25, 40, 50, 80, and 100 mg/mL sodium dodecyl sulfate (SDS). The 96-well plates were incubated for 24 h at 37 °C without shaking, and growth was verified using an ELISA reader (Molecular Devices). The MIC was determined using at least seven MIC tests per strain.

Cross-Linking Experiments and Protein Purification. The chemical cross-linking experiments were performed as previously described (*24*, *25*) with minor changes. The bacterial strains were grown to an OD_{600} of 0.5 in LB medium with appropriate antibiotic selection (50 μg/mL ampicillin and 10 μg/mL chloramphenicol) and cultivated for a further 3 h after induction of the expression plasmids. Cells were washed with 150 mM NaCl and 20 mM phosphate buffer (pH 7.4), concentrated 10-fold, and treated with 1 mM dithiobissuccinimidyl propionate (DSP) (Fluka) cross-linker at 37 °C for 30 min. The reaction was stopped with 40 mM Tris-HCl (pH 7.4). The cells were spun down and frozen and thawed repeatedly in 10 mM Tris-HCl (pH 7.4), 1 mM EDTA, and 1 mM PMSF. Lysed cells were centrifuged for 10 min at 16000*g* after addition of 10 mM $MgSO_4$. Pellets were solubilized in 8 M urea, 10 mM Tris-HCl, 100 mM NaH_2PO_4, 1% Triton X-100, and 0.2% Sarkosyl (pH 8.0) and incubated for 1 h at room temperature. After an ultracentrifugation step at 149000*g* for 30 min, the supernatants were mixed with 50 μL of Ni−NTA Sepharose resin (Amersham)/10 mL of culture and incubated overnight at 4 °C. Ni−NTA Sepharose resin was washed extensively with 8 M urea, 10 mM Tris, 100 mM imidazole, 100 mM NaH_2PO_4, and 1% Triton X-100 (pH 6.3) or 500 mM NaCl, 20 mM Tris, 100 mM imidazole, and 0.1% SDS (pH 8.0). Proteins were eluted with 8 M urea, 50 mM Tris, 2% SDS, and 700 mM imidazole (pH 4.5). The cross-linker was reduced with 80 mM dithiothreitol (DTT) for 30 min at 37 °C. As a control, the same protocol was performed in parallel without adding DSP.

For disulfide cross-linking experiments, DC14TC cells were transformed with pBADacrA$_{A93C}$B-cat and pASK-TolC or one of the two cysteine-mutant pASK-TolC plasmids in any combination. The cells were grown in 25 mL of LB medium with ampicillin, chloramphenicol, 25 ng/mL anhydrotetracycline (AHT), and 0.01% arabinose at 30 °C until an OD_{600} of 1. After the cells had been harvested by centrifugation for 15 min at 5000*g*, the pellets were resuspended in 3 mL of 10 mM Tris (pH 8.0) and 40 mM *N*-ethylmaleimide. The cells were disrupted by repeated brief sonications on ice, and cell membranes were collected by centrifugation at 170000*g* for 1 h at 4 °C. The resulting pellets were resuspended in 8 M urea before SDS−PAGE and Western blot analysis.

Resuspended membrane probes were purified using Strep-tactin Sepharose. The probes were diluted 10-fold in 100 mM Tris, 150 mM NaCl, 1 mM EDTA, and 1% Triton (pH 8) and bound overnight on Strep-tactin Sepharose. After the samples were extensively washed with 100 mM Tris, 150 mM NaCl, 1 mM EDTA, and 1% Triton (pH 8), bound TolC was eluted with 100 mM Tris, 150 mM NaCl, 1 mM EDTA, 1% Triton, and 2.5 mM desthiobiotin (pH 8). Purified TolC was examined for copurification of AcrA by Western blots after SDS−PAGE under reducing and nonreducing conditions.

SDS−PAGE and Western Blotting. Prior to electrophoresis, suspensions of approximately equal numbers of cells or dissolved aliquots of purified proteins both in sample loading buffer were heated for 10 min at 100 °C. SDS−PAGE was performed according to the Laemmli gel system (*26*). For Western blots, a tank blot system (Amersham Biosciences) was used as described previously (*27*). The anti-His and the HRP-linked anti-mouse HRP-linked anti-rabbit antibodies were purchased from Amersham Biosciences, and the AcrA specific antibody from rabbit was produced by Pineda Antibody Services (Berlin, Germany). ECL Western Blotting Detection Reagents (Amersham Biosciences) were used for detection.

Growth Curve. The bacterial strains were grown overnight in LB medium supplemented with 50 μg/mL ampicillin and 10 μg/mL chloramphenicol. Afterward, the cultures were diluted into 50 mL of fresh LB medium supplemented with 50 μg/mL ampicillin, 10 μg/mL chloramphenicol, 0.1 μM IPTG, and 0.01% arabinose, and the initial number of cells was adjusted to 5×10^7 per milliliter by measuring the OD_{600}. The OD_{600} was measured frequently, and novobiocin (final concentration of 20 μg/mL) was added when the OD_{600} reached 0.3−0.4.

Protein Modeling. The interaction model is based on the crystal structures of AcrA, MexA, TolC, and OprM (*6*, *7*, *11*, *12*). The binding sites of the channel tunnels with adaptor proteins were first identified by a bioinformatics approach (see the text) and then supported by molecular modeling using the CharmM module of InsightII (Accelrys).

RESULTS AND DISCUSSION

Construction of a Bacterial Strain with an Inducible, Cellular Regulation-Independent AcrAB/TolC Multidrug Efflux Pump. The AcrAB/TolC multidrug efflux pump is responsible for high resistance levels of *E. coli* strains against various noxious components (*28*). However, it is known that expression of the three compounds is regulated by diverse factors such as growth rate, cell density, and the presence of noxious compounds (*29*−*32*). Therefore, investigation of the interaction between components of bacterial multidrug

Table 1: Strains and Plasmids

strain	characterization	ref
AG100		*19*
AG100TC	Δ*tolC*	this work
DC14	Δ*acrAB::kan*	*19*
DC14TC	Δ*tolC*, Δ*acrAB::kan*	this work

plasmid	characterization	ref
pKD3		*20*
pACYC184	Cm^R	*22*
pGEX-3X		Amersham
pGEX-3XNdeI	NdeI cutting site in front of GST gene	this work
pNB-pre	p15 origin of replication, *cat* from pACYC184 (Cm^R), *lacI*^{q}, tac promoter, GST gene from pGEX-3X	this work
pNB1	pNB-pre + MCS (SalI-PstI-SacI-XhoI-BglII-AflII-HindIII-XmaI)	this work
pNB2	pNB-pre + MCS (XmaI-HindIII-AflII-BglII-XhoI-SacI-PstI-SalI)	this work
pBADMyc/His_C	pBR322 origin, *ara*BAD promoter, *araC*, Myc/His sequence	Invitrogen
pBADtolC	pBADMyc/His_C + *tolC*	this work
pNB1tolC	pNB1 + *tolC*, Myc/His sequence, GST gene excised	this work
pNB2tolC	pNB2 + *tolC*, Myc/His sequence, GST gene excised	this work
pNB2oprM	pNB2 + *oprM*, Myc/His sequence, GST gene excised	this work
pBADHis$_C$	pBR322 origin, araBAD promoter, *araC*, Amp^R	Invitrogen
pBADacrAB	pBADHisC + *acrAB*	this work
pUC18		*45*
pUC18acrA	pUC18 + *acrA*	this work
pUC18acrAΔHP	pUC18acrA without *acrA* hairpin sequence	this work
pUC18acrAMexAHP	pUC18acrA, *acrA* hairpin substituted with *mexA* hairpin sequence	this work
pBADacrABΔHP	pBADacrAB without *acrA* hairpin sequence	this work
pBADacrABMexAHP	pBADacrAB, *acrA* hairpin substituted with *mexA* hairpin sequence	this work
pASK-IBA12	Amp^R	IBA
pASK-TolC	pASK-IBA12 + *tolC*	this work
pASK-TolC_{S124C}	pASK-IBA12 + *tolC S124C*	this work
pASK-TolC_{S339C}	pASK-IBA12 + *tolC S339C*	this work
pBADacrAB-cat	pBADacrABΔ*bla* + *cat*, Cm^R	this work
pBADacrA_{A93C}B-cat	pBADacrAB-cat + *acrA A93C*	this work

efflux pumps by determining the minimal inhibitory concentration (MIC) requires a genetic background, which uncouples the transcription of the *tolC*, *acrA*, and *acrB* genes from cellular regulation mechanisms. We have constructed two plasmids, pBADacrAB with the *acrA* and *acrB* genes under the control of an arabinose inducible araBAD promoter, as well as pNB1tolC with *tolC* under the control of the IPTG inducible tac promoter. Both plasmids were transformed into DC14TC, an *E. coli* K12 strain with chromosomal deletions of *acrAB* and *tolC*. In MIC tests, we determined the susceptibility of strains against the antibiotics novobiocin and erythromycin, the detergents SDS and benzalkonium chloride, and the dye rhodamine 6G, all substances shown to be substrates of the AcrAB/TolC efflux pump (*28*).

First, the amounts of IPTG and arabinose were varied to determine conditions under which the MIC test revealed resistance levels for DC14TC pBADacrAB pNBtolC similar to those obtained with wild-type strain AG100 pBAD pNB. The concentrations of arabinose and IPTG for induction were set to 660 μM (=0.01%) and 0.1 μM, respectively, revealing MIC values for the reconstituted wild-type system identical to that of wild-type strain AG100 pBAD pNB. Increasing the arabinose concentration to, for example, 1320 μM resulted in higher resistance levels (>300 μg/mL for novobiocin), which is in accordance with results observed when efflux pump components were previously overexpressed (*33*). For novobiocin, we show that the absence of either TolC or AcrA and AcrB leads to high susceptibility as observed for the strain with all three proteins missing (Table 2). Interestingly, cells expressing TolC but not AcrAB were slightly more resistant to novobiocin than cells lacking TolC. The explanation for this is that TolC could also interact with other inner membrane complexes to form efflux pumps, which are able to expel novobiocin to a certain extent. The data from Sulavik and co-workers (*28*) support this interpretation, because they found that deletion of *acrAB* together with genes of four other inner membrane complexes resulted in a further reduction of resistance to novobiocin compared to single *acrAB* knockout strains. It should be mentioned that

Table 2: Minimal Inhibitory Concentrations (MICs) of Five Antimicrobial Agents for *E. coli* DC14TC Expressing Efflux Pump Components in Various Combinations[a]

		MIC (μg/mL)				
CT	AP	Nov	Ery	R6G	Benz	SDS
−	−	2.5	4.7	7.8	1.3	1250
TolC	−	7.5	nm	nm	nm	nm
−	AcrA	2.5	nm	nm	nm	nm
OprM	−	2.5	nm	nm	nm	nm
−	AcrAMexAHP	2.5	nm	nm	nm	nm
TolC	AcrAΔHP	7.5	4.7	7.8	1.3	1250
TolC	AcrA	210	200	500	16	100000
TolC	AcrAMexAHP	120	150	500	16	100000
OprM	AcrA	2.5	4.7	7.8	1.3	1250
OprM	AcrAMexAHP	80	100	375	10	50000

[a] All strains contain two plasmids: either pNB1tolC, pNB2oprM, or empty vector pNB for the IPTG-induced expression of channel tunnel (CT) genes and arabinose-induced pBAD vectors either as an empty vector or expressing AcrB together with different adaptor proteins (APs). The MIC values were determined by recording the growth of induced cultures in 96-well plates. Each value was determined using at least seven MIC tests per strain. Abbreviations: Nov, novobiocin; Ery, erythromycin; R6G, rhodamine 6G; Benz, benzalkonium chloride; SDS, sodium dodecyl sulfate.

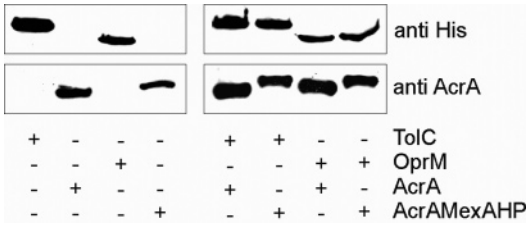

FIGURE 1: Expression of components of multidrug efflux pumps. Equal amounts of cells 3 h after induction at an OD_{600} of 0.5 with 0.01% arabinose and 0.1 μM IPTG of *E. coli* DC14TC expressing different combinations of drug efflux components were subjected to SDS−PAGE and blotted. Proteins were detected by anti-His or anti-AcrA antiserum.

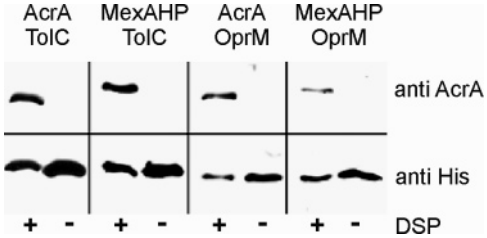

FIGURE 2: Interaction of channel tunnels and adaptor proteins proven by cross-linking. Purification of His-tagged channel proteins in the presence and absence of DSP. Copurified adaptor proteins were released by addition of DTT before SDS−PAGE and Western blotting. Proteins were detected by anti-His or anti-AcrA antiserum. AcrAMexAHP is abbreviated MexAHP.

in contrast to the araBAD promoter, which is tightly regulated, the tac promoter is leaky, which means that the presence of the pNB1tolC plasmid was sufficient to mediate resistance to a certain level even without IPTG induction. However, we induced channel tunnel expression with 0.1 μM IPTG to have a defined expression of the protein. Thus, strain DC14TC pBADacrAB pNBtolC with genes encoding the efflux pump AcrAB/TolC under control of inducible promoters provides an appropriate genetic background for studying the functionality of the protein components with MIC tests.

Components of the AcrAB/OprM Hybrid Efflux Pump Interact but Are Not Functional. To study the interaction between the inner membrane complex and the outer membrane channel, we expressed a hybrid multidrug efflux pump. Previous results show that the MexAB/OprM efflux pump of *P. aeruginosa* can be functionally expressed in *E. coli* (*34*). Thus, we used OprM to replace channel tunnel TolC in *E. coli*. Immunoblots show that the amount of OprM is slightly reduced compared to the amount of TolC, which is independent of the presence or absence of AcrAB (Figure 1). This could be explained by the fact that OprM is not a native *E. coli* protein. Cells expressing the AcrAB/OprM hybrid multidrug efflux pump were susceptible to the tested drugs with MIC values comparable to that of the TolC deficient strain. Even stronger induction of OprM did not increase the resistance of the cells (data not shown). This shows clearly that OprM is not functional with AcrAB, which supports previous reports (*35*).

In the next step, we tried to find out if the hybrid efflux pump is not functional because the AcrAB inner membrane complex of *E. coli* and the channel tunnel of *P. aeruginosa* did not assemble. Copurification of AcrA with OprM after chemical cross-linking shows that the hybrid efflux pump components are in contact (Figure 2). This means that the inner and outer components of the hybrid efflux pump can interact but that this interaction is not sufficient to form a functional efflux pump. Similar results were shown recently for another hybrid efflux pump composed of *E. coli* AcrAB and outer membrane channel VceC of *Vibrio cholerae*. The proteins physically interact as shown by chemical cross-linking experiments, but they do not form a functional efflux pump (*36*).

Exchange of AcrA with the MexA Hairpin Confers Functionality of the AcrAB/OprM Hybrid Efflux Pump. Almost all models of efflux pumps assume that the hairpin subdomain of the adaptor protein makes contact with the outer membrane component (*10*, *14*, *37*). The importance of the hairpin was shown by an AcrA mutant. Seventy-four residues (97−170), forming the hairpin, were replaced by the DPG tripeptide, resulting in the AcrAΔHP mutant. When it was expressed together with AcrB and TolC, the amount of AcrAΔHP detected by immunoblotting was more than 100-fold lower compared to the amount of wild-type AcrA (data not shown), and the construct failed to mediate resistance (Table 2). This suggests that deletion of the hairpin domain destabilizes the protein, explaining why the efflux pump is not functional. The instability of AcrAΔHP explains also why the protein could not be copurified with TolC after chemical cross-linking (data not shown). Similar observations were made with a carboxy-terminal deletion mutant of AcrA (*12*). However, we can exclude the possibility that contact with the outer membrane component is necessary for correct folding of the adaptor protein. The protein level of wild-type AcrA is not reduced in a TolC deficient background (Figure 1).

On the basis of the observation that interaction of AcrAB with OprM is not sufficient to form a functional drug efflux pump, we constructed an AcrA adaptor protein with the hairpin replaced with the MexA hairpin. We used a 218 bp PCR fragment comprising the MexA hairpin and the adjacent regions of the lipoyl domain of AcrA as primers in a QuikChange PCR. It allowed a precise exchange of the hairpin without introducing new residues. This was important because initial hairpin exchange attempts, by ligation of the *mexA* hairpin sequence into self-created restriction sites in *acrA*, led to point mutations resulting in a less stable protein and reduced MIC levels (data not shown). Western blot analysis shows that the amount of mutant protein (denoted AcrAMexAHP) is slightly reduced compared to the amount of wild-type AcrA protein, which is independent of the presence or absence of TolC or OprM (Figure 1). Unexpectedly, the hybrid protein had an apparently higher molecular weight. However, we confirmed that it is the mature form of AcrAMexAHP by overexpressing the proteins, which revealed an additional band with a higher molecular weight corresponding to the unprocessed form (data not shown). Interaction of the chimeric protein with TolC as well as OprM was proven by copurification after chemical cross-linking (Figure 2).

Although it is known that the MexAB/TolC hybrid efflux pump is not functional in *E. coli* (*34*, *35*), coexpression of the AcrAMexAHP mutant with AcrB and TolC establishes a resistance phenotype. This means that TolC tolerates the exchange of the AcrA hairpin with the MexA hairpin. When the AcrAMexAHP chimeric adaptor protein was expressed

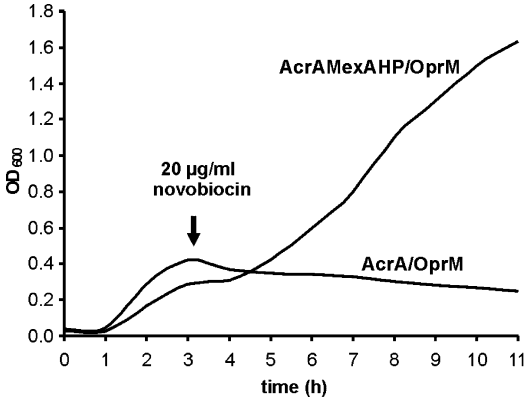

FIGURE 3: Effect of novobiocin on the growth of cells expressing OprM in combination with wild-type AcrA or AcrAMexAHP. Protein expression was induced with 0.1 μM IPTG and 0.01% arabinose from the beginning. Novobiocin was added to final concentration of 20 μg/mL when the OD_{600} reached 0.3−0.4.

with AcrB and OprM, the MIC values for all tested compounds were significantly increased compared to those of cells expressing the AcrAB/OprM hybrid efflux pump (Table 2). The resistance level did not reach that of the AcrAB/TolC efflux pump. This might be explained to a certain extent by the amounts of OprM and AcrAMexAHP being slightly smaller than the amounts of TolC and AcrA, respectively. However, the experiment clearly shows that the exchange of the AcrA hairpin with the MexA hairpin makes OprM useful for a functional efflux pump.

This result was also further confirmed by a susceptibility test in a liquid culture. When novobiocin was added to an exponential culture expressing AcrAB/OprM (final concentration of 20 μg/mL), the growth stopped immediately as observed for cells lacking at least one efflux pump component (Figure 3). In contrast, the addition of novobiocin to cells expressing OprM and AcrB with AcrAMexAHP led to a short lag time followed by continuous growth. Taken together, our results show that the exchange of the AcrA hairpin with that of MexA is sufficient to change the AcrAB/OprM hybrid efflux pump from a nonfunctional into a functional export machinery.

Model for MexAHP−OprM Interaction. The crystal structure of OprM shows that the periplasmic entrance of OprM is almost closed (*6*), and it is obvious and already shown for TolC that it needs to be open to allow export (*38*). It is believed that opening is induced by specific interaction with the inner membrane complex (*7*, *39*). Our results show that the exchange of the MexA hairpin is sufficient to convert the nonfunctional AcrAB/OprM hybrid efflux pump into functional export machinery. Therefore, we assume that the MexA hairpin inherits the ability to open OprM tunnel entrance. Since structural information about OprM and MexA is available, several models of efflux pumps are proposed. Exceptional is the model of Gerken and Misra suggesting that the position of the adaptor protein is shifted toward the outer membrane in a way that the α/β-domain of the adaptor protein interacts directly with the tunnel (*18*). This assumption supports their interpretation of a direct interaction of these two domains. However, isothermal titration calorimetry experiments argue against a direct interaction of the α/β-domain with the tunnel (*40*). Another argument against the model of Gerken and Misra is that the hairpins include the equatorial domain, therefore making a direct interaction of the hairpins with the tunnel-forming helices impossible. All other models agree that the hairpin interacts with the tunnel helices. However, the models differ in the oligomeric state of the adaptor protein proposing trimers, hexamers, or nonamers (*10*, *14*, *37*). On the basis of a detailed analysis of the structures, we describe the first model for interaction between the channel and the adaptor protein on a molecular level. We assume that six adaptor proteins interact with the tunnel domain. This assumption is supported by biochemical evidence of a 2:1:1 stoichiometry for the MexAB/OprM efflux pump components (*41*).

Channel tunnels have evolved most likely by gene duplication events, deduced from sequence homology between the amino- and carboxy-terminal halves (*42*, *43*). To characterize residues that are involved in interaction with MexA, we have determined the amino acids at the tunnel domain of OprM, which are conserved in both halves of the protein, indicating that they are part of the MexA binding site (colored light yellow in Figure 4). It is not surprising that leucine and valine residues at the interface between two adjacent helices are conserved, since they play a role in maintaining the tunnel structure. However, there are also conserved hydrophobic residues facing outward. A region close to the periplasmic end comprises conserved aromatic residues located in helices H3 and H7. Conserved valine and leucine residues further contribute to a hydrophobic surface of H7 and H8 and of H3 and H4, respectively. Charged residues, which are conserved, are rather rare. There are just three residues all located in the more outward-facing helices H3 and H7. When the residues on the MexA hairpin are examined, it is striking that the surface of the downward helix (Hdown) on the opposite side of the lipoyl and β-barrel domain is covered by small residues such as glycine, alanine, and serine (colored black). These residues are often found in helices with close contacts with other proteins. The only charged residues at this side of the MexA hairpin are two aspartate residues. When the MexA hairpin and the OprM structure are brought together in a way that Hdown interacts with the hydrophobic patch between the H7 and H8 and H3 and H4 helix pairs, respectively, the structures fit perfectly in both cases. Salt bridges can be formed between the conserved positively charged residues in helices H3 and H7 and the negative charges on the hairpin surface. An arginine residue at the side of Hup comes close to the negatively charged conserved residue in helices H3 and H7 and could also form a salt bridge (Figure 4, circled residues). Other charged residues on the surface of the OprM tunnel come close to asparagine and glutamine residues, allowing interaction via hydrogen bonds. It should be noted that no equally charged residues would face each other in this model, which means that there are no repelling forces. We assume that this perfect assembly of the hairpins with the tunnel helices is a prerequisite for induction of the conformational change which opens the tunnel entrance. Primarily, the proper interaction of the MexA hairpin with the binding site formed by H7, H8, and H3 might be important for induction of the outward movement of the inner coiled coils formed by H7 and H8.

It should be mentioned that in the case of the nonfunctional hybrid efflux pump AcrAB/VceC functionality could be restored by gain of function mutants of VceC (*36*). Here,

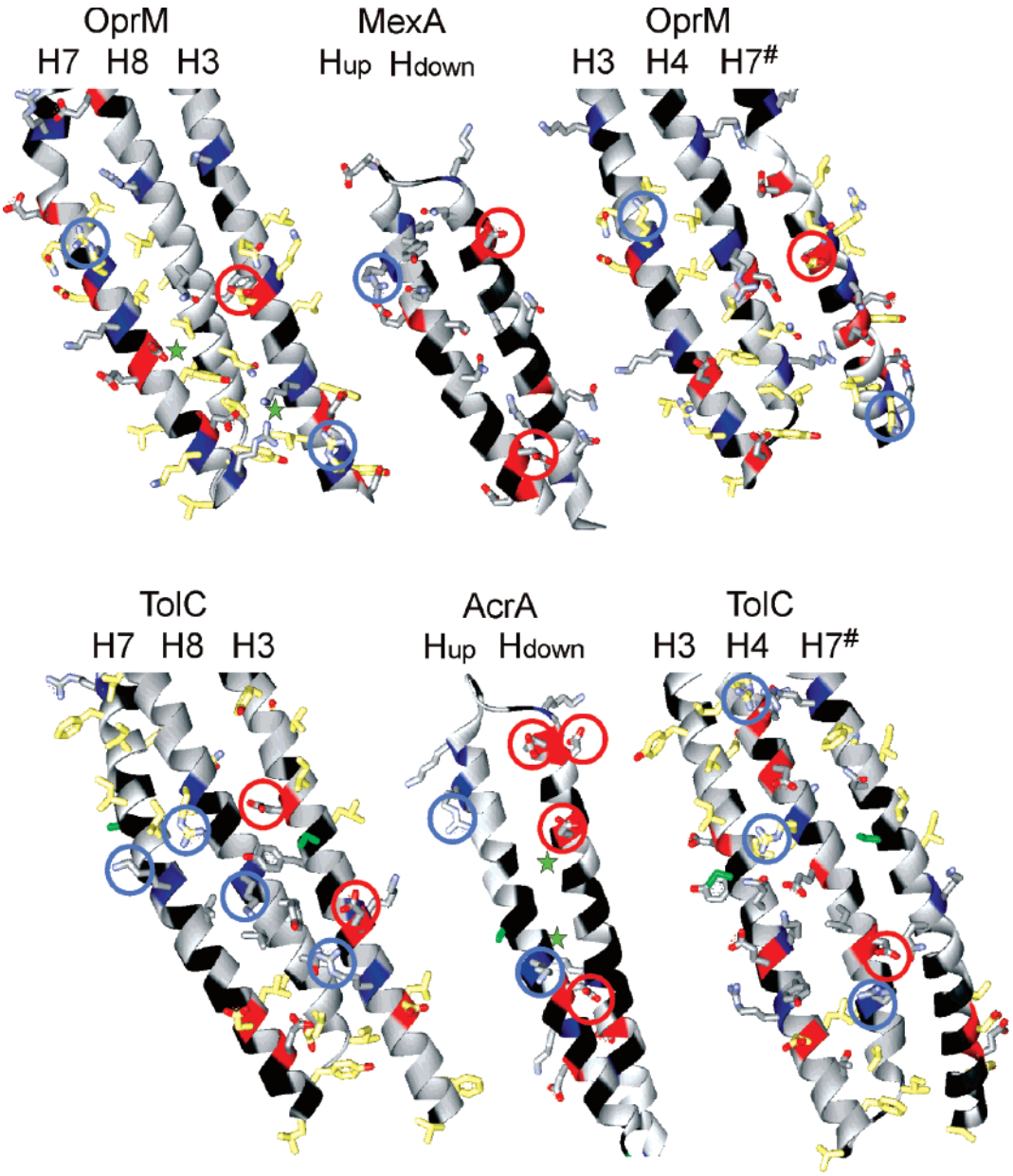

FIGURE 4: Structures of channel tunnel helices forming the tunnel domain below the equatorial domain and adaptor protein hairpins. The channel tunnel structures are split for clarity. The helix pairs H7 and H8 and H3 and H4 are shown with the adjacent helix of the same protomer (H3) and of the adjacent protomer (H7#). The adaptor protein hairpins are shown in an orientation with the lipoyl and β-barrel domain facing backward. Side chains of residues, which are conserved in both halves of channel tunnels, are colored light yellow. The helices are colored black at positions with small side chains (glycine, alanine, and serine), red at positions with negatively charged residues, and blue at positions with positively charged residues. The circles denote residues which might form salt bridges for channel tunnel−adaptor protein interaction. Residues which conflict in the assembling of AcrA with OprM are marked with green stars. Residues substituted with cysteine in AcrA and TolC are colored green. For further explanation, see the text. The following PDB entries were used: 1WP1 (OprM), 1EK9 (TolC), 1VF7 (MexA), and 2F1M (AcrA).

single-point mutations in VceC made it possible that the AcrAB inner membrane complex is able to functionally interact with VceC. It is thought that the gain of function mutants provide functionality, because they are able to undergo the transition into or persist in an open state when in association with the AcrAB complex. The localization and nature of the mutated residues, which are in part predicted to face into the tunnel lumen, support the possibility that most probably the destabilization of the closed state of the VceC tunnel is the reason for the gain of function and not the improved interaction with the inner membrane complex as suggested for the AcrAMexAHPAcrB/OprM hybrid efflux pump.

The Interaction Model Explains the Incompatibility of AcrA and OprM. In contrast to MexA hairpins, AcrA hairpins are not able to functionally interact with OprM. Bringing the AcrA and OprM structures together explains why the interaction is not functional (Figure 4). There are two major differences between the hairpin of MexA and AcrA. First, the surface of AcrA, which interacts most likely with the tunnel helices, is covered by three more charged residues than the surface of MexA. The additional charges do not conflict when AcrA is assembled with the H3/H4/H7# hairpin binding site of OprM. This might explain why even AcrA and OprM interact as shown by cross-linking experiments. When trying to model the binding of AcrA to the H7/H8/

H3 hairpin binding site of OprM, which might be crucial for opening the tunnel entrance, we find there is a conflict due to repelling charges (marked with a green star). The second difference between the AcrA and MexA hairpins is the size of the hairpin. The AcrA hairpin is 11 Å longer due to seven additional residues per helix. Assuming that at least the H3/H4/H7# hairpin binding site of OprM binds AcrA, the longer extension of the AcrA hairpin leads to a gap between the end of the tunnel and the top of the transporter.

Recently, it was shown for TolC and AcrB by disulfide cross-linking that there is close contact between the two proteins (*9*). Because it might be possible that the interaction between the channel and the RND transporter is also necessary for a functional efflux pump, the missing contact between OprM and AcrB could also contribute to the failure of the AcrAB/OprM hybrid efflux pump.

AcrAMexAHP Is Compatible with TolC. In our AcrAMexAHP/AcrB/TolC hybrid efflux pump, there is functional interaction between the MexA hairpin and TolC. This could be explained by the fact that the MexA hairpin is covered by very few charged residues, which do not conflict with charges on the potential hairpin binding sites of TolC, even though the hairpin is two helical turns shorter than that of AcrA. One must also consider that TolC serves as outer membrane component of diverse export machineries, requiring an interaction site which is compatible with very distinct hairpin domains. Additionally, when the tunnel domains of TolC and OprM are compared, it is obvious that OprM is more tightly closed than TolC. Therefore, a less specific interaction with the hairpin could be sufficient for a functional efflux pump. Furthermore, in this hybrid efflux pump, the TolC channel tunnel assembles with its native RND transporter AcrB, which might facilitate tunnel opening mediated by the MexA hairpin. The incompatibility of MexAB with TolC (*35*) is another hint that besides the interaction with the hairpin interaction with the RND transporter is necessary for a functional efflux pump.

Model for AcrA−TolC Interaction. In a manner similar to that for OprM and MexA, we have modeled the interaction between AcrA and TolC (Figure 4). When the charge distribution of the AcrA hairpin is examined, it fits perfectly to residues at the TolC tunnel surface of helices H7, H8, and H3. Six salt bridges can be formed, when the AcrA hairpin assembles with this part of the TolC tunnel (circled residues). Like the surface of Hdown of MexA, the surface of Hdown of AcrA is covered with small residues, which agrees well with the hydrophobic area between H7 and H8 of TolC. The mode of interaction of the AcrA hairpin with the second binding site formed by H3, H4, and H7# is slightly different. In contrast to H3, there are no charged residues at H7#, which could interact with AcrA. However, corresponding charged groups are found at H4, which could form salt bridges with residues in the middle of Hup. Small residues at the surface of H7# and at Hup allow a close contact of the two proteins. As in the assembly of AcrA with TolC H7/H8/H3, there are no electrostatic conflicts in the assembly with H3/H4/H7#, which means that the AcrA model seems reasonable. It should be noted that the AcrA structure determination revealed a conformational flexibility of the AcrA hairpin domain (*12*). Recently, a comparable flexibility was also predicted for MexA (*44*). This observation is in good agreement with the idea of a hexameric adaptor protein.

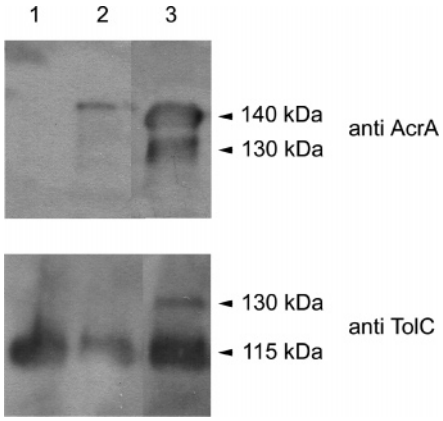

FIGURE 5: Western blot analysis of membrane fractions resuspended in 8 M urea of DC14TC cells expressing AcrAA93C in combination with wild-type TolC (lane 1), TolCS124C (lane 2), or TolCS339C (lane 3). Samples were mixed with nonreducing loading buffer and incubated at 100 °C for 10 min prior to 6% SDS−PAGE. TolC and AcrA were detected with α-TolC and α-AcrA antibodies (Pineda Antibody Services, Berlin, Germany), respectively.

The orientation of the helices forming the two distinct interaction sites on the tunnel surface is a little different due to the different curling of the inner and outer coiled coil. Thus, the flexibility of the hairpin makes docking at two distinct interaction sites on the tunnel surface possible. Furthermore, the flexibility also allows a hingelike rearrangement of the hairpin domain, which is necessary for the conformational change of the tunnel helices for opening of the periplasmic entrance (*14*).

Validation of the Interaction Model by Site-Directed Disulfide Cross-Linking. The general interaction between channel tunnels and adaptor proteins could already be proven repeatedly by chemical cross-linking for TolC and AcrA (*15*, *17*, *40*). Models of the multidrug efflux pumps assume that the hairpin interacts with the inner coiled coils to induce opening and stabilize the open configuration (*10*, *11*, *37*). We could confirm this assumption by restoring the resistance phenotype of susceptible TolC mutants with reverted charges at the inner coiled coils by AcrA mutants with exchanged charges at the corresponding positions of the hairpin (G. Polleichtner et al., manuscript in preparation). For validation of the second interaction site comprising the outer coiled coils, we have identified the residues serine 339 of TolC and alanine 93 of AcrA, which are in the proximity of each other during the modeled interaction. The TolC cysteine mutant TolCS124C was constructed as negative control, because according to our model the distance between cysteine 93 at the AcrA hairpin and the position of cysteine 124 of TolC is too far for them to become covalently linked. Membrane fractions of (urea-treated) cells expressing AcrAA93C in combination with wild-type TolC, TolCS124C, or TolCS339C were loaded under nonreducing conditions on a SDS gel, and AcrA and TolC were detected by Western blots. Both proteins were detected in a monomeric and dimeric form. It should be noted that the dimers of both proteins had an apparent molecular mass higher that what was expected, 140 kDa for TolC and 115 kDa for AcrA (Figure 5). The same observations were made for TolC cysteine mutants by Tamura et al. (*9*). As expected, the combinations of TolCS339C and AcrAA93C showed additional bands for both TolC and AcrA at 130 kDa,

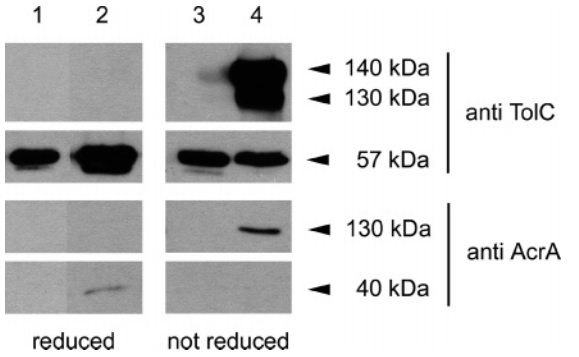

FIGURE 6: Western blot analysis of elution probes of strep tag-purified membrane extractions of DC14TC cells expressing AcrAA93C with wild-type TolC (lanes 1 and 3) or TolCS339C (lanes 2 and 4). Samples were mixed with reducing or nonreducing loading buffer and incubated at 100 °C for 10 min prior to 7% SDS−PAGE. TolC and AcrA were detected with α-TolC and α-AcrA antibodies (Pineda Antibody Services), respectively.

respectively, and this intermediate mass points toward cross-linked TolC−AcrA complexes. To prove this assumption, the resuspended membrane probes were purified using Strep-tactin Sepharose. Purified TolCS339C was examined for copurification of AcrA in Western blot analysis. In fact, AcrA could be detected together with TolCS339C, while no AcrA can be detected for the equally treated control strains with wild-type TolC (Figure 6). Additionally, analyzing the elution samples under nonreducing conditions, we find the complex band at 130 kDa again can be detected with AcrA and TolC antibodies. If this is transferred to the model, this means that our assumption of a second interaction site comprising the outer coiled coils is correct. There are two AcrA interaction sites at the tunnel surface of a TolC protomer.

CONCLUSION

We have elucidated the role of the hairpin domain for the assembling and function of efflux pumps. However, the mechanism of drug efflux remains to be elucidated. Prerequisite is the understanding of the efflux pump assembly. Integrating our experimental data and structural analysis, we have presented the first detailed model of the interaction between the adaptor protein and channel tunnel of two different efflux pumps. The cysteine mutants covalently linking outer and inner membrane components make copurification and crystallization of the complete drug efflux machinery possible. Knowledge of the binding sites will also help in designing efflux drug inhibitors needed to combat multiresistant bacterial strains.

ACKNOWLEDGMENT

We thank W. V. Kern for providing us with *E. coli* strains AG100 and DC14 and R. McCorkell for correcting the manuscript.

SUPPORTING INFORMATION AVAILABLE

Table of oligonucleotides. This material is available free of charge via the Internet at http://pubs.acs.org.

REFERENCES

1. Cosgrove, S. E., and Carmeli, Y. (2003) The impact of antimicrobial resistance on health and economic outcomes, *Clin. Infect. Dis. 36*, 1433−1437.
2. Zgurskaya, H. I., and Nikaido, H. (2000) Multidrug resistance mechanisms: Drug efflux across two membranes, *Mol. Microbiol. 37*, 219−225.
3. Poole, K. (2001) Multidrug resistance in Gram-negative bacteria, *Curr. Opin. Microbiol. 4*, 500−508.
4. Andersen, C., Hughes, C., and Koronakis, V. (2001) Protein export and drug efflux through bacterial channel-tunnels, *Curr. Opin. Cell Biol. 13*, 412−416.
5. Andersen, C. (2003) Channel-tunnels: Outer membrane components of type I secretion systems and multidrug efflux pumps of Gram-negative bacteria, *Rev. Physiol. Biochem. Pharmacol. 147*, 122−165.
6. Akama, H., Kanemaki, M., Yoshimura, M., Tsukihara, T., Kashiwagi, T., Yoneyama, H., Narita, S., Nakagawa, A., and Nakae, T. (2004) Crystal structure of the drug discharge outer membrane protein, OprM, of *Pseudomonas aeruginosa*: Dual modes of membrane anchoring and occluded cavity end, *J. Biol. Chem. 279*, 52816−52819.
7. Koronakis, V., Sharff, A., Koronakis, E., Luisi, B., and Hughes, C. (2000) Crystal structure of the bacterial membrane protein TolC central to multidrug efflux and protein export, *Nature 405*, 914−919.
8. Murakami, S., Nakashima, R., Yamashita, E., and Yamaguchi, A. (2002) Crystal structure of bacterial multidrug efflux transporter AcrB, *Nature 419*, 587−593.
9. Tamura, N., Murakami, S., Oyama, Y., Ishiguro, M., and Yamaguchi, A. (2005) Direct interaction of multidrug efflux transporter AcrB and outer membrane channel TolC detected via site-directed disulfide cross-linking, *Biochemistry 44*, 11115−11121.
10. Akama, H., Matsuura, T., Kashiwagi, S., Yoneyama, H., Narita, S., Tsukihara, T., Nakagawa, A., and Nakae, T. (2004) Crystal structure of the membrane fusion protein, MexA, of the multidrug transporter in *Pseudomonas aeruginosa*, *J. Biol. Chem. 279*, 25939−25942.
11. Higgins, M. K., Bokma, E., Koronakis, E., Hughes, C., and Koronakis, V. (2004) Structure of the periplasmic component of a bacterial drug efflux pump, *Proc. Natl. Acad. Sci. U.S.A. 101*, 9994−9999.
12. Mikolosko, J., Bobyk, K., Zgurskaya, H. I., and Ghosh, P. (2006) Conformational flexibility in the multidrug efflux system protein AcrA, *Structure 14*, 577−587.
13. Johnson, J. M., and Church, G. M. (1999) Alignment and structure prediction of divergent protein families: Periplasmic and outer membrane proteins of bacterial efflux pumps, *J. Mol. Biol. 287*, 695−715.
14. Fernandez-Recio, J., Walas, F., Federici, L., Venkatesh, P. J., Bavro, V. N., Miguel, R. N., Mizuguchi, K., and Luisi, B. (2004) A model of a transmembrane drug-efflux pump from Gram-negative bacteria, *FEBS Lett. 578*, 5−9.
15. Husain, F., Humbard, M., and Misra, R. (2004) Interaction between the TolC and AcrA proteins of a multidrug efflux system of *Escherichia coli*, *J. Bacteriol. 186*, 8533−8536.
16. Mokhonov, V. V., Mokhonova, E. I., Akama, H., and Nakae, T. (2004) Role of the membrane fusion protein in the assembly of resistance-nodulation-cell division multidrug efflux pump in *Pseudomonas* aeruginosa, *Biochem. Biophys. Res. Commun. 322*, 483−489.
17. Tikhonova, E. B., and Zgurskaya, H. I. (2004) AcrA, AcrB, and TolC of *Escherichia coli* Form a Stable Intermembrane Multidrug Efflux Complex, *J. Biol. Chem. 279*, 32116−32124.
18. Gerken, H., and Misra, R. (2004) Genetic evidence for functional interactions between TolC and AcrA proteins of a major antibiotic efflux pump of *Escherichia coli*, *Mol. Microbiol. 54*, 620−631.
19. Jellen-Ritter, A. S., and Kern, W. V. (2001) Enhanced expression of the multidrug efflux pumps AcrAB and AcrEF associated with insertion element transposition in *Escherichia coli* mutants selected with a fluoroquinolone, *Antimicrob. Agents Chemother. 45*, 1467−1472.
20. Datsenko, K. A., and Wanner, B. L. (2000) One-step inactivation of chromosomal genes in *Escherichia* coli K-12 using PCR products, *Proc. Natl. Acad. Sci. U.S.A. 97*, 6640−6645.
21. Sambrook, J., Fritsch, E. F., and Maniatis, T. (1988) *Molecular Cloning: A Laboratory Manual*, 2nd ed., Cold Spring Harbor Laboratory Press, Plainview, NY.
22. Rose, R. E. (1988) The nucleotide sequence of pACYC184, *Nucleic Acids Res. 16*, 355.
23. Geiser, M., Cebe, R., Drewello, D., and Schmitz, R. (2001) Integration of PCR fragments at any specific site within cloning

vectors without the use of restriction enzymes and DNA ligase, *BioTechniques 31*, 88−90, 92.
24. Balakrishnan, L., Hughes, C., and Koronakis, V. (2001) Substrate-triggered recruitment of the TolC channel-tunnel during type I export of hemolysin by *Escherichia coli*, *J. Mol. Biol. 313*, 501−510.
25. Zgurskaya, H. I., and Nikaido, H. (2000) Cross-linked complex between oligomeric periplasmic lipoprotein AcrA and the inner-membrane-associated multidrug efflux pump AcrB from *Escherichia coli*, *J. Bacteriol. 182*, 4264−4267.
26. Laemmli, U. K. (1970) Cleavage of structural proteins during the assembly of the head of bacteriophage T4, *Nature 227*, 680−685.
27. Towbin, H., Staehelin, T., and Gordon, J. (1979) Electrophoretic transfer of proteins from polyacrylamide gels to nitrocellulose sheets: Procedure and some applications, *Proc. Natl. Acad. Sci. U.S.A. 76*, 4350−4354.
28. Sulavik, M. C., Houseweart, C., Cramer, C., Jiwani, N., Murgolo, N., Greene, J., DiDomenico, B., Shaw, K. J., Miller, G. H., Hare, R., and Shimer, G. (2001) Antibiotic susceptibility profiles of *Escherichia coli* strains lacking multidrug efflux pump genes, *Antimicrob. Agents Chemother. 45*, 1126−1136.
29. Miller, P. F., and Sulavik, M. C. (1996) Overlaps and parallels in the regulation of intrinsic multiple-antibiotic resistance in *Escherichia coli*, *Mol. Microbiol. 21*, 441−448.
30. Rahmati, S., Yang, S., Davidson, A. L., and Zechiedrich, E. L. (2002) Control of the AcrAB multidrug efflux pump by quorum-sensing regulator SdiA, *Mol. Microbiol. 43*, 677−685.
31. Rand, J. D., Danby, S. G., Greenway, D. L., and England, R. R. (2002) Increased expression of the multidrug efflux genes acrAB occurs during slow growth of *Escherichia coli*, *FEMS Microbiol. Lett. 207*, 91−95.
32. Rosenberg, E. Y., Bertenthal, D., Nilles, M. L., Bertrand, K. P., and Nikaido, H. (2003) Bile salts and fatty acids induce the expression of *Escherichia coli* AcrAB multidrug efflux pump through their interaction with Rob regulatory protein, *Mol. Microbiol. 48*, 1609−1619.
33. Augustus, A. M., Celaya, T., Husain, F., Humbard, M., and Misra, R. (2004) Antibiotic-sensitive TolC mutants and their suppressors, *J. Bacteriol. 186*, 1851−1860.
34. Srikumar, R., Kon, T., Gotoh, N., and Poole, K. (1998) Expression of *Pseudomonas aeruginosa* multidrug efflux pumps MexA-MexB-OprM and MexC-MexD-OprJ in a multidrug-sensitive *Escherichia coli* strain, *Antimicrob. Agents Chemother. 42*, 65−71.
35. Tikhonova, E. B., Wang, Q., and Zgurskaya, H. I. (2002) Chimeric analysis of the multicomponent multidrug efflux transporters from Gram-negative bacteria, *J. Bacteriol. 184*, 6499−6507.
36. Vediyappan, G., Borisova, T., and Fralick, J. A. (2006) Isolation and characterization of VceC gain-of-function mutants that can function with the AcrAB multiple-drug-resistant efflux pump of *Escherichia coli*, *J. Bacteriol. 188*, 3757−3762.
37. Eswaran, J., Koronakis, E., Higgins, M. K., Hughes, C., and Koronakis, V. (2004) Three's company: Component structures bring a closer view of tripartite drug efflux pumps, *Curr. Opin. Struct. Biol. 14*, 741−747.
38. Eswaran, J., Hughes, C., and Koronakis, V. (2003) Locking TolC entrance helices to prevent protein translocation by the bacterial type I export apparatus, *J. Mol. Biol. 327*, 309−315.
39. Andersen, C., Koronakis, E., Bokma, E., Eswaran, J., Humphreys, D., Hughes, C., and Koronakis, V. (2002) Transition to the open state of the TolC periplasmic tunnel entrance, *Proc. Natl. Acad. Sci. U.S.A. 99*, 11103−11108.
40. Touze, T., Eswaran, J., Bokma, E., Koronakis, E., Hughes, C., and Koronakis, V. (2004) Interactions underlying assembly of the *Escherichia coli* AcrAB-TolC multidrug efflux system, *Mol. Microbiol. 53*, 697−706.
41. Narita, S., Eda, S., Yoshihara, E., and Nakae, T. (2003) Linkage of the efflux-pump expression level with substrate extrusion rate in the MexAB-OprM efflux pump of *Pseudomonas aeruginosa*, *Biochem. Biophys. Res. Commun. 308*, 922−926.
42. Andersen, C., Hughes, C., and Koronakis, V. (2000) Chunnel vision. Export and efflux through bacterial channel-tunnels, *EMBO Rep. 1*, 313−318.
43. Gross, R. (1995) Domain structure of the outer membrane transporter protein CyaE of *Bordetella* pertussis, *Mol. Microbiol. 17*, 1219−1220.
44. Vaccaro, L., Koronakis, V., and Sansom, M. (2006) Flexibility in a drug transport accessory protein: Molecular dynamics simulations of MexA, *Biophys. J. 91*, 558−564.
45. Yanisch-Perron, C., Vieira, J., and Messing, J. (1985) Improved M13 phage cloning vectors and host strains: Nucleotide sequences of the M13mp18 and pUC19 vectors, *Gene 33*, 103−119.

BI060320G